

Published in final edited form as:

*Gastroenterology*. 2013 June ; 144(7): 1543–1553.e1. doi:10.1053/j.gastro.2013.02.037.

## Hippo Signaling Regulates Differentiation and Maintenance in the Exocrine Pancreas

Tao Gao<sup>1,4</sup>, Dawang Zhou<sup>5,6</sup>, Chenghua Yang<sup>1,4</sup>, Tarjinder Singh<sup>1</sup>, Alfredo Penzo-Méndez<sup>1,4</sup>, Ravikanth Maddipati<sup>1,4</sup>, Alexandros Tzatsos<sup>5</sup>, Nabeel Bardeesy<sup>5</sup>, Joseph Avvruch<sup>5</sup>, and Ben Z. Stanger<sup>1,2,3,4,\*</sup>

<sup>1</sup>Gastroenterology Division, Department of Medicine, University of Pennsylvania School of Medicine, Philadelphia, PA 19104, USA

<sup>2</sup>Department of Cell and Developmental Biology, University of Pennsylvania School of Medicine, Philadelphia, PA 19104, USA

<sup>3</sup>Abramson Family Cancer Research Institute, University of Pennsylvania School of Medicine, Philadelphia, PA 19104, USA

<sup>4</sup>Abramson Cancer Center, University of Pennsylvania School of Medicine, Philadelphia, PA 19104, USA

<sup>5</sup>The Massachusetts General Hospital, Harvard Medical School, Boston, MA 02114, USA

<sup>6</sup>State Key Laboratory of Stress Cell Biology, School of Life Sciences, Xiamen University, Xiamen, Fujian 361005, China

### Abstract

**BACKGROUND & AIMS**—The Hippo signaling pathway is a context-dependent regulator of cell proliferation, differentiation, and apoptosis in species ranging from *Drosophila* to humans. In this study, we investigated the role of the core Hippo kinases—Mst1 and Mst2—in pancreatic development and homeostasis.

**METHODS**—We used a Cre/LoxP system to create mice with pancreas-specific disruptions in *Mst1* and *Mst2* (*Pdx1-Cre;Mst1<sup>-/-</sup>;Mst2<sup>fl/fl</sup>* mice), the mammalian orthologs of *Drosophila Hippo*. We used a transgenic approach to overexpress Yap, the downstream mediator of Hippo signaling, in the developing pancreas of mice.

**RESULTS**—Contrary to expectations, the pancreatic mass of *Pdx1-Cre;Mst1<sup>-/-</sup>;Mst2<sup>fl/fl</sup>* mice was reduced compared with wild-type mice, largely because of postnatal de-differentiation of acinar cells into duct-like cells. Development of this phenotype coincided with postnatal reactivation of YAP expression. Ectopic expression of YAP during the secondary transition (a

© 2013 The American Gastroenterological Association. Published by Elsevier Inc. All rights reserved.

\*Corresponding author: 421 Curie Boulevard, Perelman School of Medicine, University of Pennsylvania, Philadelphia, PA 19104; 215-746-5560; bstanger@exchange.upenn.edu.

**Publisher's Disclaimer:** This is a PDF file of an unedited manuscript that has been accepted for publication. As a service to our customers we are providing this early version of the manuscript. The manuscript will undergo copyediting, typesetting, and review of the resulting proof before it is published in its final citable form. Please note that during the production process errors may be discovered which could affect the content, and all legal disclaimers that apply to the journal pertain.

**Author Contributions:** Study concept and design (TG, NB, JA, BZS); data acquisition (TG, CY, AP-M, RM); analysis and interpretation of data (TG, TS, AP-M, RM, AT, NB, JA, BZS); statistical analysis (TG, TS, AT); drafting the manuscript (TG, BZS); obtained funding (BZS).

**Conflicts of Interest:** None

Author names in bold designate shared co-first authorship.

stage at which YAP is normally absent) blocked differentiation of the endocrine and exocrine compartments, whereas loss of a single *Yap* allele reduced acinar de-differentiation. The phenotype of *Pdx1-Cre;Mst1<sup>-/-</sup>;Mst2<sup>fl/fl</sup>* mice recapitulated cellular and molecular changes observed during chemical-induced pancreatitis in mice.

**CONCLUSIONS**—The mammalian Hippo kinases, and YAP, maintain postnatal pancreatic acinar differentiation in mice.

## Keywords

mouse model; signal transduction; Hpo; Wts

## Introduction

In *Drosophila*, the Hippo signaling pathway is composed of two core kinases, Hippo (*Hpo*) and Warts (*Wts*), which function to inactivate the downstream effector, Yorkie (*Yki*). In the presence of active kinases, phosphorylated Yorkie remains inactive in the cytoplasm, while in the absence of Hpo or Wts, unphosphorylated Yorkie moves into nucleus and activates transcription<sup>1</sup>. The Hippo pathway is highly conserved from *Drosophila* to mammals, with most components having multiple orthologs identified in mammals<sup>2</sup>. One conserved component of the pathway is Hippo itself, a serine-threonine kinase which shares high sequence similarity with its functionally-redundant mammalian orthologs *Mst1* and *Mst2*<sup>3</sup>. Deletion of the genes encoding *Mst1* and *Mst2* in rodent models leads to severe context-dependent phenotypes. In the liver, *Mst1/2* loss leads to organ growth<sup>4-6</sup>, whereas *Mst1/2* deletion in the intestine leads to over-proliferation of intestinal stem cells and colonic tumorigenesis<sup>7</sup>.

The pancreas is a close developmental relative of the liver, and the ventral pancreas and liver share a bi-potential progenitor cell population within embryonic endoderm<sup>8</sup>. Given the fact that dysregulation of Hippo signaling causes dramatic effects on liver development and postnatal growth, we sought to determine whether the Hippo kinases are also involved in pancreas development and size regulation. To this end, we took advantage of a Cre/loxP system to delete *Mst1* and *Mst2* in the developing mouse pancreas.

## Methods and Materials

### Animals

We used a Cre/LoxP system to specifically delete *Mst1* and *Mst2* in the pancreatic epithelium. *Mst1<sup>-/-</sup>* and *Mst2<sup>fl/fl</sup>* mice<sup>6</sup> were bred to *Pdx1-Cre* mice<sup>9</sup> to create *Pdx1-Cre; Mst1<sup>-/-</sup>; Mst2<sup>fl/fl</sup>* (DKO) mice. BrdU labeling experiments were performed by administering 100 mg/kg body weight of BrdU IP two hours before sacrifice. Results are representative of 6–7 animals in either control or mutant groups unless otherwise indicated. Control animals were littermates of the genotype *Pdx1-Cre; Mst1<sup>+/-</sup>; Mst2<sup>fl/+</sup>* except in microarray experiments, in which the control animals were of the genotype *Pdx1-Cre; Mst1<sup>-/-</sup>; Mst2<sup>fl/+</sup>* (this was done to minimize microarray effects based on litter/cage given the design of the breeding strategy). The *Elastase-CreER* strain has been previously reported<sup>10</sup>. In *Yap1* transgenic over-expression studies, littermate embryos that lacked either the *Yap* or rtTA transgene were used as controls.

For the generation of *Yap*-deficient mice, BAC recombineering was used to introduce loxP sites into the 5' UTR and first intron of the mouse *Yap1* gene along with an upstream PGK-neo selection cassette. The resulting construct was linearized and injected into V6.5 ES cells, which were screened for positive clones by southern blot analysis. Chimeric mice were

generated by injection of two independently correctly targeted clones into blastocysts. Upon confirmation of germ-line transmission, chimeric mice were bred to FLPase mice (The Jackson laboratory) to delete the neo-cassette. The resulting mice were determined to be null (or severely hypomorphic) for *Yap1* based on the failure to obtain homozygous offspring but normal rates of birth for heterozygous “*Yap<sup>het</sup>*” animals.

For the generation of YAP-inducible mice, site directed mutagenesis was used to introduce a serine-to-alanine amino acid substitution at position 112 of the murine YAP1 protein; this mutation has been reported previously to promote nuclear translocation and activation of YAP protein<sup>1, 11</sup>. To facilitate cell lineage tracing, a GFP coding cassette was ligated in-frame to the 3' end of the *Yap1* coding region linked by a viral 2A peptide, permitting simultaneous transcription of *Yap1* and *GFP* from a bicistronic template. This coding region was placed downstream from a tetracycline response element (pTight, Clontech) and cloned into the PacI and AscI sites of a pROSA26A targeting vector backbone. This construct was linearized with *SwaI*, electroporated into V6.5 ES cells, and correctly targeted ES cell clones were confirmed by southern blot. Chimeric mice were generated by independent blastocyst injection of two correctly targeted clones. The resulting tetO-YAP-GFP mice were bred to *ROSA-rtTA* mice (The Jackson Laboratory). The YAP-GFP transgene was induced by giving pregnant mice 2mg/ml doxycycline in in sucrose-supplemented drinking water from E13.5 to E17.5. Pregnant mice were sacrificed at E17.5 and embryos were harvested for further analysis. For developmental studies, the morning of the vaginal plug was considered embryonic day 0.5. All animal experiments were performed in accordance with NIH policies on the use of laboratory animals and approved by the IACUC of the University of Pennsylvania.

### Histological Analysis and Immunostaining

Liver and pancreas tissues were fixed in 4% paraformaldehyde overnight at 4°C followed by paraffin embedding. Paraffin sections from each sample were cut at 5 µm. H&E and immunostaining were performed as previously described<sup>6</sup>. ABC kit (Vector Laboratories) was used for immunohistochemical applications as described previously<sup>6</sup>. TUNEL assay was performed with *In Situ* Cell Death Detection Kit (Roche). Quantification of BrdU and TUNEL was performed by counting positive cells at 20× magnification (BrdU) or 40× magnification (TUNEL) by fluorescent microscopy. *P*-values were calculated by Student's *t*-test.

### Microarray and Quantitative RT-PCR (qPCR) Analysis

Seven day-old pups were sacrificed and pancreata immediately taken out and homogenized in Qiazol (Qiagen). Total RNA was extracted from pancreas by using an RNeasy total RNA isolation Kit (Qiagen) according to manufacturer's protocol. 500ng of total RNA were used for the synthesis of cDNA, followed by amplification and biotin labeling. A total of 1.5 µg of biotinylated cRNA was hybridized to the Mouse Gene 1.0ST microarray. After staining with streptavidin-phycoerythrin and biotinylated anti-streptavidin, samples were scanned and using GCS3000 laser scanner collected data. All statistical analyses were performed using Ingenuity Pathway Analysis database and under the R language environment. A heat map of expression was generated by Treeview<sup>13</sup>. Differentially expressed genes in control versus Hippo pathway mutant tissues are displayed in Supplementary Figure 5 and listed in Supplementary Table 1. Quantitative RT-PCR analysis was carried out using SYBR green gene expression assays (QIAGEN) according to the manufacturer's instructions. Microarray data have been deposited in the NCBI GEO database with accession number GSE44298 (<http://www.ncbi.nlm.nih.gov/geo/query/acc.cgi?acc=GSE44298>).

## Results

### Intact Hippo signaling is required for normal pancreatic morphology

To assess the role of Hippo signaling during pancreatic development, we used the Pdx1-Cre strain to specifically delete *Mst1* and *Mst2* in the developing pancreatic epithelium. This strain mediates deletion as early as embryonic day 9<sup>14</sup>. Mutant mice were born at Mendelian ratios and appeared healthy. Western blot showed effective deletion of both *Mst1* and *Mst2* in pancreata from 30 day-old double knockout (“DKO”) mice, which was accompanied by an increase in the abundance of total YAP and a relative decrease in the abundance of phospho-YAP (Fig. 1A). Surprisingly, pancreas-specific deletion of *Mst1/2* resulted in an approximately 2-fold decrease in pancreas mass (Fig. 1B). This finding was in sharp contrast to the overgrowth phenotype in mice with hepatic deletion of *Mst1/2* (Supplementary Fig. 1; refs. 4–6).

Hematoxylin and eosin (H&E) staining showed extensive histological abnormalities characterized by acinar cell atrophy and an expansion of duct-like cells (Fig. 1C i,v). To characterize the exocrine compartment of the mutant pancreas, we co-stained for the ductal marker cytokeratin 19 (CK19) and the acinar marker carboxypeptidase 1 (CPA1). Compared to littermate controls, DKO mutant pancreata exhibited a decrease in CPA1<sup>+</sup> acinar cells, an increase of CK19<sup>+</sup> duct cells, and numerous “double positive” cells (Fig. 1C ii, vi (inset), D). In the endocrine compartment, we stained for markers of  $\beta$  cells (Ins) and  $\alpha$  cells (Gluc). *Mst1/2* loss resulted in a disruption of islet architecture and a significant increase in the ratio of  $\alpha$  to  $\beta$  cells (Fig. 1C iii, vii, 1E). Consistent with the western blot results, *Mst1/2* deletion resulted in an increase in the number of YAP-expressing cells in the pancreas; YAP staining was confined to the ducts of control mice (Fig. 1C iv), whereas YAP<sup>+</sup> cells exhibiting nuclear staining were found throughout DKO pancreata (Fig. 1C viii).

The architectural abnormalities and changes in cell ratios observed in the endocrine compartment of DKO mice prompted us to ask whether *Mst1/2* loss had physiological consequences. Surprisingly, 1 month-old DKO mice were euglycemic and had a normal response to glucose challenge (Supplementary Fig. 2A). When we double-stained pancreata for YAP and C-peptide, YAP staining was not detected in the  $\beta$ -cells of either control or DKO animals, suggesting that islets do not express YAP (Supplementary Fig. 2B iii). Consistent with this lack of YAP expression, TUNEL and BrdU staining failed to reveal a difference in islet cell proliferation or survival in DKO animals compared to controls (Supplementary Fig. 2B iii–vi).

### Pancreatic abnormalities are acquired postnatally in *Mst1/2* mutant animals

To address the mechanism for the decreased pancreas size in DKO mice, we examined mutant and control animals for cell proliferation and cell death. In contrast to the endocrine compartment, the exocrine compartment of DKO mice exhibited a significant increase in cell proliferation, as indicated by BrdU staining (Fig. 2A, C). In addition, mutant pancreata also exhibited more cell death by TUNEL staining (Fig. 2B, C). Given the role of Hippo signaling in regulating stem cell pools, we stained for the markers Sox9 and Hes1, which mark pancreatic progenitor cells as well as ducts. Mutant pancreata exhibited strong staining for both of these markers (Fig. 2D, E), a finding that was further confirmed by Western blotting (Fig. 2F).

We reasoned that two general mechanisms might account for the observed ductal metaplasia phenotype in DKO pancreata. First, there could be a failure of exocrine maturation, in which pancreas progenitor cells might be blocked from acquiring a terminally differentiated acinar identity. Alternatively, acinar cells could develop normally and subsequently undergo a loss of acinar identity, causing them to become duct-like cells. To distinguish between these



possibilities, we performed a series of time-course and lineage-tracing studies in which pancreata were analyzed at different time points during development, from embryonic day 15.5 (E15.5) through postnatal P14.

DKO animals exhibited normal pancreatic mass through P14, with a decrease in size becoming apparent only at P30 (Fig. 3A). Analysis of pancreatic histology revealed no abnormalities in DKO animals at E15.5 and P0 (Fig. 3E i, ii, v,vi), with only a fraction displaying metaplasia at P7 and all animals exhibiting metaplasia by P14 (Fig. 3E iii, iv, vii, viii). Co-immunofluorescence with CK19 and CPA provided further confirmation of this time-course, with acinar atrophy and ductal expansion becoming apparent at approximately P7 (Fig. 3E ix–xvi). “Double positive” cells – cells which expressed both acinar and ductal markers – were also first apparent at P7 (Fig. 3E xv, inset). qPCR for acinar-specific transcription factors revealed normal transcript levels for *Mist1*, *Ptf1a*, *RBP-JL*, and *Lrh1* in DKO animals at P0 (Fig. 3D), suggesting that DKO pancreata had adopted a normal acinar program at birth. Taken together, these results suggest that acinar cells can differentiate in the absence of *MST1* and *MST2* but then fail to retain their differentiated phenotype.

To determine whether the timing of ductal metaplasia could be attributed to the normal temporal regulation of Hippo pathway components, we used western blotting to examine the expression of *MST1*, *MST2*, and *YAP* over the course of embryonic and postnatal pancreas development. While *MST1* and *YAP* (but not *MST2*) proteins were detected in control pancreata at E15.5, their expression was almost undetectable at P0 before returning to higher levels at P7 and P14 (Fig. 3B and Supplementary Fig. 3A). In DKO animals, *MST1* and *MST2* were absent or markedly reduced at all time-points examined. Of note, *Mst1/2* deficiency had no effect on *YAP* protein levels in the embryonic pancreas, whereas *Mst1/2* deficiency was associated with higher levels of total *YAP* at P7 and P14 (Fig. 3B). As described for P30 (Fig. 1A), this increase in total *YAP* was associated with a decrease in the relative abundance of P-*YAP* (data not shown). We also performed real time PCR to assess the transcription of pathway components. *Mst1* mRNA was absent and *Mst2* mRNA was significantly decreased at all time-points (Fig. 3C), consistent with our western blot results and suggesting that DKO embryos lack *Mst1/2* early in development. Interestingly, *YAP* mRNA levels did not change between control and DKO at any time point (Fig. 3C), consistent with the notion that most of *MST1/2*'s effects on *YAP* are post-translational.

We then immunostained for *YAP* at various time-points during pancreas development. In control pancreata, nuclear *YAP* staining was observed in the “trunk” regions of the pancreatic epithelium at E15.5 (Fig. 3E xvii) before becoming undetectable at birth (Fig. 3E xviii); at P7 and later stages, *YAP* expression was confined mainly to the ductal compartment (Fig. 3E xix, xx; Fig. 1C iv; Fig. 5B i; Supplementary Fig. 2). By contrast, abundant *YAP* staining was observed in pancreata from P7 and P14 DKO mice, where it was found in the abnormal duct-like structures in these animals (Fig. 3E xxiii, xxiv).

### ***Mst1/2* loss promotes acinar de-differentiation**

The abundance of “double positive” cells (co-expressing CK19 and CPA1) led us to hypothesize that the postnatal expansion of duct-like cells in DKO mice is due to the loss of acinar identity. Alternatively, duct cell proliferation (due to *Pdx1*-Cre-mediated deletion of *Mst1/2* in duct cells) could underlie the phenotype. In order to distinguish between these possibilities, we generated *ElastaseCreER*, *Mst1*<sup>-/-</sup>; *Mst2*<sup>fl/fl</sup>; *Rosa*<sup>YFP</sup> (EKO) mice, in which tamoxifen could be used to induce acinar-specific deletion of *Mst1/2*. The *ElastaseCreER* strain has previously been shown to mediate acinar-specific recombination<sup>10</sup> and we confirmed this specificity using the *Rosa*<sup>YFP</sup> lineage tracer (Supplementary Fig. 3B). Three weeks after administering tamoxifen, strong *YAP* expression was detected in EKO *YFP*<sup>+</sup> acinar cells (Supplementary Fig. 3Biii, inset) and a fraction of these cells had acquired

a duct-like morphology and expressed the ductal marker CK19 (Supplementary Fig. 3C), suggesting that the duct-like cells in DKO mice were directly descended from acinar cells. In addition, we performed co-immunofluorescence staining of control and DKO pancreata at P7 and P14, in which DKO pancreata showed abundant YAP/CPA1 double positive cells, further confirming the conversion of acinar cells to a duct-like phenotype (Supplementary Fig. 3D).

To further rule out the possibility that the pancreatic phenotype in DKO animals was due simply to duct cell proliferation, we quantified the percentage of CK19 duct cells that also stained positive for the proliferation marker Ki67. At P0 and P7, there was no significant difference between control and DKO animals (Supplementary Fig. 4). Taken together, these results suggest that in the absence of *Mst1/2*, acinar cells differentiate normally but fail to maintain their differentiated state and de-differentiate or trans-differentiate into a duct-like state.

### **Yap lies downstream of *Mst1/2* in the pancreas**

In *Drosophila*, Hippo signaling results in a transcriptional readout that is mediated by the *Yap* ortholog *Yki*. To determine whether *Yap* lies downstream of the mammalian Hippo kinases, we performed an epistasis analysis by breeding mice with a single null allele of *Yap1* onto the DKO background (resulting in DKO; *YAP<sup>het</sup>* mice; Fig. 4B). Four weeks after birth, five out of twelve DKO; *YAP<sup>het</sup>* animals exhibited a dramatic improvement in pancreatic histology (Fig. 4A, C), demonstrating that disruption of a single allele of YAP is sufficient to phenotypically rescue a fraction of *Mst1/2* mutant animals. Hence, we conclude that YAP is a major mediator of signaling resulting from *Mst1/2* loss in the pancreas.

### **Ectopic expression of YAP during late gestation interferes with pancreatic differentiation**

Our expression analysis demonstrated that YAP is absent during the late embryonic and perinatal periods, raising the possibility that YAP must be silenced for proper pancreas differentiation. Alternatively, cells in the embryonic pancreas may not be competent to respond to YAP signals, in which case the perinatal repression of MST1, MST2, and YAP seen in control mice might be merely incidental. To address this question, we created a mouse model in which a constitutive active form of YAP could be ectopically expressed in a regulated fashion. TetO-YAP-GFP mice were made by placing a bicistronic construct containing an activated form of mouse YAP (S112A) and a GFP label downstream of tetracycline regulatory elements (Fig. 5A). When crossed to mice expressing the reverse tetracycline transactivator (rtTA) under control of the Rosa26 promoter, the resulting double transgenic mice exhibited doxycycline-inducible expression of YAP and GFP in pancreatic epithelial cells and some mesenchymal cells (Fig. 5B, C). Treatment of mice with doxycycline from E13.5 to 17.5 resulted in a marked expansion of the ductal compartment at the expense of acinar cells (Fig. 5B v, vi, D) and endocrine cells (Fig 5B vii, viii, E). Hence, embryonic cells remain competent to respond to YAP signaling late in pancreatic development, and repression of YAP is necessary for normal acinar and endocrine differentiation.

### ***Mst1/2* mutants phenocopy the histologic changes of acute pancreatitis**

Because the phenotype of P30 *Mst1/2* DKO animals resembled that observed in models of acute pancreatitis<sup>15</sup>, we sought to address a potential relationship between Hippo signaling and pancreatitis. To this end, we induced acute pancreatitis (AP) in 30 day-old mice using the cholecystokinin analog caerulein and compared the phenotypes caused by AP and *Mst1/2* deletion. Pancreata exposed to caerulein exhibited a dramatic increase in CK19<sup>+</sup> ductal structures and a decrease in CPA1<sup>+</sup> acinar structures, reminiscent of the DKO phenotype (Fig. 6A i–vi). These changes were associated with strong YAP induction (Fig.

6B, C). Conversely, several proteins known to be induced in AP – including PDX1, SOX9, Clusterin, and  $\beta$ -catenin – were also observed in DKO pancreata (Fig. 6A vii–xv).

The similarity between the DKO and AP phenotypes raised the possibility that the changes seen in DKO mice might be a secondary consequence of pancreatitis caused by *Mst1/2* deletion. To address this possibility, we examined the timing of acinar cell death and immune infiltration in mutant animals. At postnatal day 7, a time point when histologic evidence of ductal metaplasia was already present, there was no increase in cell death by TUNEL staining or immune infiltration by CD45 staining (Supplementary Fig. 5). A week later, at P14, cell death and immune cell infiltration were both increased in DKO mice (Supplementary Fig. 5). This result indicates that acinar de-differentiation precedes cell death and the appearance of pancreatitis.

Finally, we performed a microarray analysis at P7 comparing control and DKO animals. Two hundred and one genes were differentially regulated ( $>1.5\times$  fold-change) with a step-up *P*-value of less than 0.05 (Supplementary Fig. 6A). Notably, 85% of the differentially-expressed genes were up-regulated, indicating that MST1/2 (acting at least in part through YAP) has an overall repressive effect on gene expression. Among the differentially-expressed genes were those that act as immune mediators, such as prostaglandin synthase (Ptgds) and stromal-derived factor 1 (SDF1/CXCL2; Supplementary Fig. 6B, C). In addition, DKO animals exhibited deregulation of genes involved in integrin signaling and cell adhesion (Supplementary Fig. 6B, C). Thus, *Mst1/2* loss is associated the activation of a programs predicted to drive changes in cell morphology and to promote leukocyte invasion.

## Discussion

Hippo signaling has recently emerged as an evolutionarily conserved pathway involved in embryonic cell fate decisions, organ growth, and cancer<sup>16, 17</sup>. The transcriptional and functional output of this signal is highly context dependent, resulting in effects as divergent as the inner cell mass vs. trophectoderm cell fate decision<sup>18</sup> and enhanced liver cell proliferation and survival<sup>4–6</sup>. Here, we have shown that elimination of both *Mst1* and *Mst2* from the pancreas results in a paradoxical decrease in pancreas size caused by a YAP-dependent loss of acinar cell identity that resembles the acinar response to acute pancreatitis.

Normal pancreatic differentiation occurs in two waves: the “primary transition” (~E10), during which there is a modest increase in the production of pancreatic hormones, and the “secondary transition” (~E14–16), during which there is a dramatic increase in the production of digestive enzymes and hormones. Following the secondary transition, newly specified acinar cells undergo further maturation and expansion before acquiring a fully differentiated morphology<sup>19</sup>. We found that MST1 and YAP, but not MST2, are normally present during the secondary transition. However, both of these kinases, and YAP itself, are absent at birth, only to reappear in the first two weeks of postnatal life. Ectopic expression of *Yap* during the secondary transition (E13.5–E17.5) disrupted pancreatic development, interfering with both acinar and endocrine differentiation. These observations support the hypothesis that YAP is permissive for pancreatic development during mid-gestation but that it must be repressed during or immediately after the secondary transition for maturation to occur. Similar findings have been recently reported by George et al.,<sup>20</sup> who showed that metaplasia following pancreatic *Mst1/2* deletion also occurs after the completion of exocrine differentiation. Consistent with this notion, *Yap* induction in the adult pancreas is sufficient to promote ductal metaplasia<sup>11</sup>.

Surprisingly, *Mst1/2* deletion had no effect on YAP expression or phosphorylation at E15.5 or postnatal day 1, indicating that perinatal YAP repression occurs through an *Mst1/2*-

independent mechanism. By contrast, *Mst1/2* deletion resulted in a marked increase in total YAP abundance at postnatal day 7 and subsequent time-points, as well as an associated decrease in the relative abundance of P-YAP. Notably, *Mst1/2* deletion in the liver had no effect on total YAP levels, but resulted in a dramatic decrease in the amount of P-YAP.

In mammals, at least two Lats1/2-associated phosphorylation events have been reported to regulate YAP protein activity: phosphorylation of S127, which results in binding to 14-3-3 proteins and cytoplasmic sequestration, and phosphorylation of S381, which results in ubiquitination and degradation<sup>(16, 21)</sup>. As *Mst1/2* regulate Lats activity, deletion of *Mst1/2* could be expected to have effects on YAP phosphorylation status, YAP abundance, or both. Our results indicate that both mechanisms are employed during pancreatic development, in contrast to the liver where phosphorylation seems to be the dominant mechanism.

Our findings also provide an explanation for the timing of the mutant phenotype in DKO animals, in which loss of acinar differentiation becomes apparent only as mutant animals exhibit detectable differences in YAP expression at postnatal day 7. Together, our observations support a model in which *Mst1* and *Mst2* regulate postnatal YAP levels and phosphorylation status in acinar cells to maintain differentiation (Fig. 7). Although this model is supported by lineage tracing experiments and the appearance of “intermediate” cells with shared acinar/ductal features, we cannot entirely rule out the possibility that part of the *Mst1/2* mutant phenotype is due to ductal (or centroacinar) expansion, which might have also contributed to the increase of YAP expression in DKO pancreata.

We found that the introduction of a single mutant *Yap* allele into the *Mst1/2* mutant background rescues the phenotype in nearly half of DKO mutants, demonstrating that this phenotype requires YAP. In both the intestine and liver (as in the pancreas), loss of a single *Yap* allele is sufficient to rescue the phenotype resulting from either *Mst1/2* or *Nf2* loss<sup>7,22</sup>. Thus, MST1/2 signaling is highly sensitive to *Yap* gene dosage in several tissues.

Because the pancreatic histology of DKO mice resembled that seen following acute pancreatitis (AP), we sought to determine whether these two processes might be linked. We found that AP led to an induction of markers that are also upregulated in DKO mutants, including YAP, HES1, and SOX9. Conversely, deletion of *Mst1* and *Mst2* resulted in the induction of proteins known to be associated with acute pancreatitis, including PDX1, Clusterin, and  $\beta$ -catenin. Thus, *Mst1/2* loss phenocopies AP. Importantly, loss of acinar cell identity in the context of *Mst1/2* deletion is not a secondary outcome of pancreatitis, as cell death and immune cell infiltration are first observed at postnatal day 14, well after metaplasia has occurred. Hence, in the setting of *Mst1/2* deletion, immune infiltration is a consequence rather than a cause of the acinar changes. Our microarray revealed a number of genes that are upregulated at postnatal day 7 – prior to leukocyte infiltration – that could be contributing to immune cell recruitment. Further studies will be needed to determine the precise role of Hippo signaling during AP.

Several important questions remain regarding the role of Hippo in pancreatic development and homeostasis, including the identity of the upstream signals that regulate the pathway and the downstream transcriptional output that mediates its effects. Hippo signaling is thought to be initiated by heterotypic interactions between atypical cadherins on neighboring cells that act as a sensor for cell density<sup>23</sup>. Thus, it is possible that as they grow and mature, acinar cells undergo an increase in pathway activation (through the activity of MST1 and MST2), resulting in YAP repression and maintenance of the mature acinar state. Similarly, it remains unclear how pathway inactivation, and increased YAP activity, leads to changes in acinar differentiation. In our microarray comparison of control and *Mst1/2* mutant pancreata, the vast majority of differentially regulated genes were upregulated in the mutant, suggesting

that YAP is acting almost exclusively as an activator of gene transcription in the pancreas. Surprisingly, gene ontology analysis suggested that *Mst1/2* deletion resulted in altered expression of genes involved in cell migration or cell adhesion (Supplementary Fig. 6). Thus, Hippo signaling may lead first to changes in cell shape and adhesion and only subsequently to changes in cellular identity.

## Acknowledgments

We are grateful to Charlie Murtaugh and Joe Kissil for comments on the manuscript and helpful suggestions. We thank Doug Melton for providing Pdx1-Cre and Elastase-CreER mice and Klaus Kaestner for providing Foxa3-Cre mice. We are grateful to Nicholas George and Nora Sarvetnick for sharing unpublished work. We thank Jenny Hu, the AFCRI morphology core, the Penn Digestive Disease Center Morphology Core, and the Penn Microarray core for technical assistance.

**Funding:** This work was supported by grants from NIH/NIDDK (DK083355 and DK083111), the Penn Center for Molecular Studies in Digestive and Liver Diseases (P30-DK050306), the Pew Charitable Trusts, and the Abramson Family Cancer Research Institute.

## Reference

- Dong JX, Feldmann G, Huang JB, Wu S, Zhang NL, Comerford SA, Gayyed MF, Anders RA, Maitra A, Pan DJ. Elucidation of a universal size-control mechanism in Drosophila and mammals. *Cell*. 2007; 130:1120–1133. [PubMed: 17889654]
- Halder G, Johnson RL. Hippo signaling: growth control and beyond. *Development*. 2011; 138:9–22. [PubMed: 21138973]
- Dan I, Watanabe NM, Kusumi A. The Ste20 group kinases as regulators of MAP kinase cascades. *Trends in Cell Biology*. 2001; 11:220–230. [PubMed: 11316611]
- Lu L, Li Y, Kim SM, Bossuyt W, Liu P, Qiu Q, Wang YD, Halder G, Finegold MJ, Lee JS, Johnson RL. Hippo signaling is a potent in vivo growth and tumor suppressor pathway in the mammalian liver. *Proceedings of the National Academy of Sciences of the United States of America*. 2010; 107:1437–1442. [PubMed: 20080689]
- Song H, Mak KK, Topol L, Yun KS, Hu JX, Garrett L, Chen YB, Park O, Chang J, Simpson RM, Wang CY, Gao B, Jiang J, Yang YZ. Mammalian Mst1 and Mst2 kinases play essential roles in organ size control and tumor suppression. *Proceedings of the National Academy of Sciences of the United States of America*. 2010; 107:1431–1436. [PubMed: 20080598]
- Zhou DW, Conrad C, Xia F, Park JS, Payer B, Yin Y, Lauwers GY, Thasler W, Lee JT, Avruch J, Bardeesy N. Mst1 and Mst2 Maintain Hepatocyte Quiescence and Suppress Hepatocellular Carcinoma Development through Inactivation of the Yap1 Oncogene. *Cancer Cell*. 2009; 16:425–438. [PubMed: 19878874]
- Zhou DW, Zhang YY, Wu H, Barry E, Yin Y, Lawrence E, Dawson D, Willis JE, Markowitz SD, Camargo FD, Avruch J. Mst1 and Mst2 protein kinases restrain intestinal stem cell proliferation and colonic tumorigenesis by inhibition of Yes-associated protein (Yap) overabundance. *Proceedings of the National Academy of Sciences of the United States of America*. 2011; 108:E1312–E1320. [PubMed: 22042863]
- Deutsch G, Jung JN, Zheng MH, Lora J, Zaret KS. A bipotential precursor population for pancreas and liver within the embryonic endoderm. *Development*. 2001; 128:871–881. [PubMed: 11222142]
- Gu GQ, Dubauskaite J, Melton DA. Direct evidence for the pancreatic lineage: NGN3+ cells are islet progenitors and are distinct from duct progenitors. *Development*. 2002; 129:2447–2457. [PubMed: 11973276]
- Stanger BZ, Stiles B, Lauwers GY, Bardeesy N, Mendoza M, Wang Y, Greenwood A, Cheng KH, McLaughlin M, Brown D, DePinho RA, Wu H, Melton DA, Dor Y. Pten constrains centroacinar cell expansion and malignant transformation in the pancreas. *Cancer Cell*. 2005; 8:185–195. [PubMed: 16169464]
- Camargo FD, Gokhale S, Johnnidis JB, Fu D, Bell GW, Jaenisch R, Brummelkamp TR. YAP1 increases organ size and expands undifferentiated progenitor cells. *Current Biology*. 2007; 17:2054–2060. [PubMed: 17980593]



12. Zong Y, Panikkar A, Xu J, Antoniou A, Raynaud P, Lemaigre F, Stanger BZ. Notch signaling controls liver development by regulating biliary differentiation. *Development*. 2009; 136:1727–1739. [PubMed: 19369401]
13. Eisen MB, Spellman PT, Brown PO, Botstein D. Cluster analysis and display of genome-wide expression patterns. *Proceedings of the National Academy of Sciences of the United States of America*. 1998; 95:14863–14868. [PubMed: 9843981]
14. Gu GQ, Brown JR, Melton DA. Direct lineage tracing reveals the ontogeny of pancreatic cell fates during mouse embryogenesis. *Mechanisms of Development*. 2003; 120:35–43. [PubMed: 12490294]
15. Sivere JT, Lubeseder-Martellato C, Lee M, Mazur PK, Nakhai H, Radtke F, Schmid RM. Notch signaling is required for exocrine regeneration after acute pancreatitis. *Gastroenterology*. 2008; 134:544–555. [PubMed: 18242220]
16. Pan D. The hippo signaling pathway in development and cancer. *Dev Cell*. 2010; 19:491–505. [PubMed: 20951342]
17. Avruch J, Zhou D, Fitamant J, Bardeesy N. Mst1/2 signalling to Yap: gatekeeper for liver size and tumour development. *British Journal of Cancer*. 2011; 104:24–32. [PubMed: 21102585]
18. Nishioka N, Inoue K-i, Adachi K, Kiyonari H, Ota M, Ralston A, Yabuta N, Hirahara S, Stephenson RO, Ogonuki N, Makita R, Kurihara H, Morin-Kensicki EM, Nojima H, Rossant J, Nakao K, Niwa H, Sasaki H. The Hippo Signaling Pathway Components Lats and Yap Pattern Tead4 Activity to Distinguish Mouse Trophoctoderm from Inner Cell Mass. *Developmental Cell*. 2009; 16:398–410. [PubMed: 19289085]
19. Pan FC, Wright C. Pancreas Organogenesis: From Bud to Plexus to Gland. *Developmental Dynamics*. 2011; 240:530–565. [PubMed: 21337462]
20. George NM, Day CE, Boerner BP, Johnson RL, Sarvetnick NE. Hippo signaling regulates pancreas development through inactivation of Yap. *Mol Cell Biol*. 2012; 32:5116–5128. [PubMed: 23071096]
21. Zhao B, Tumaneng K, Guan KL. The Hippo pathway in organ size control, tissue regeneration and stem cell self-renewal. *Nat Cell Biol*. 2011; 13:877–883. [PubMed: 21808241]
22. Zhang N, Bai H, David KK, Dong J, Zheng Y, Cai J, Giovannini M, Liu P, Anders RA, Pan D. The Merlin/NF2 Tumor Suppressor Functions through the YAP Oncoprotein to Regulate Tissue Homeostasis in Mammals. *Developmental Cell*. 2010; 19:27–38. [PubMed: 20643348]
23. Schlegelmilch K, Mohseni M, Kirak O, Pruszk J, Rodriguez JR, Zhou D, Kreger BT, Vasioukhin V, Avruch J, Brummelkamp TR, Camargo FD. Yap1 Acts Downstream of alpha-Catenin to Control Epidermal Proliferation. *Cell*. 2011; 144:782–795. [PubMed: 21376238]

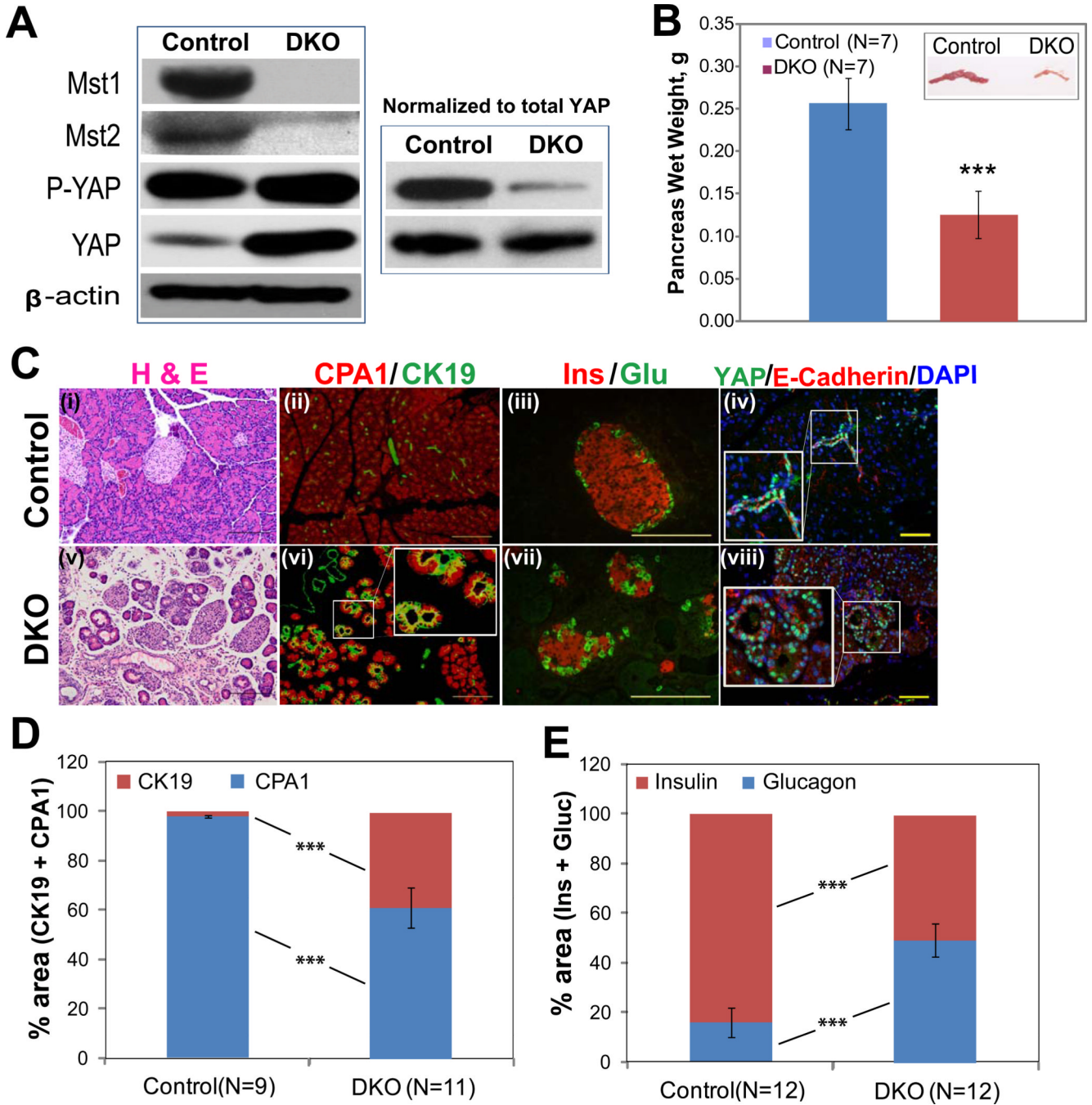


**Figure 1. Pancreatic deletion of Mst1 and Mst2 results in increased nuclear YAP, decreased pancreas size, and altered pancreatic architecture**

(A) Western blot showing the relative abundance of Mst1, Mst2, phospho-YAP (P-YAP), and total YAP in protein extracts from 1-month-old control (Pdx1-Cre; Mst1<sup>+/-</sup>; Mst2<sup>fl/+</sup>) or DKO pancreas (Pdx1-Cre; Mst1<sup>-/-</sup>; Mst2<sup>fl/fl</sup>). In the left-hand panel, 30  $\mu$ g of total protein was loaded in each lane; in the right-hand panel, loading was adjusted so an equal amount of total YAP was loaded to each lane. Blots are representative of three independent experiments.

(B) Bar graph showing pancreas weight from control and DKO animals (mean  $\pm$  SD; \*\*\*,  $P < 0.01$ ). Inset: photograph of control and DKO pancreata.

(C) H&E and immuno-staining of control and DKO pancreata with cytokeratin 19 (CK19), carboxypeptidase A1 (CPA1), insulin (Ins), glucagon (Glu) and YAP shows a disruption of pancreatic architecture and cell types in DKO pancreas and an increased abundance of cells exhibiting nuclear YAP staining.

(D, E) Quantification of changes in relative percentage of acinar/ductal area (D; measured by CPA1 and CK19 staining) and  $\alpha/\beta$  area (E; measured by insulin and glucagon staining) in control versus DKO pancreata (mean  $\pm$  SD; \*\*\*,  $P < 0.001$ ). Scale: 100  $\mu$ M.

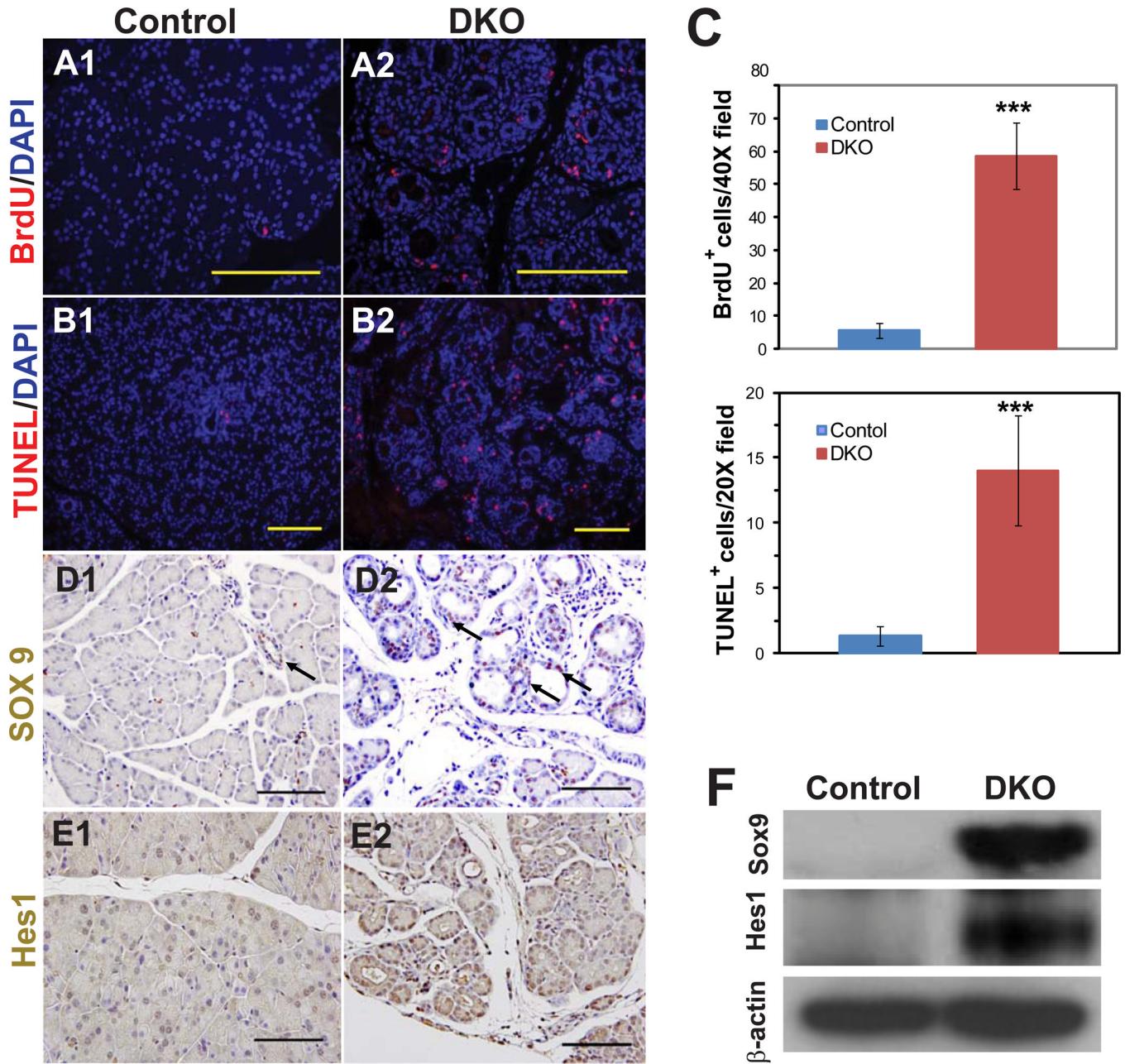


**Figure 2. *Mst1* and *Mst2* mutant pancreata exhibit increased cell turnover and upregulation of Sox9 and Hes1**

(A, B) Immunostaining of pancreata from 1 month-old DKO or littermate control for BrdU (cell proliferation; A1, A2) or TUNEL reactivity (cell death; B1, B2).

(C) Quantification of data from (A, B), showing a marked increase in both cell proliferation and cell death in DKO mice. Data were obtained from four mice in each group, with two to three fields counted for each mouse (mean  $\pm$  SD; \*\*\*,  $P < 0.001$ ).

(D, E) Immunostaining of pancreata from control or DKO animals for Sox9 (D1, D2) or Hes1 (E1, E2).

(F) Western blot using antibodies against Sox9 and Hes1;  $\beta$  actin served a loading control. Blot is representative of 3 mutant-control pairs tested. Scale bar: 100  $\mu$ M.



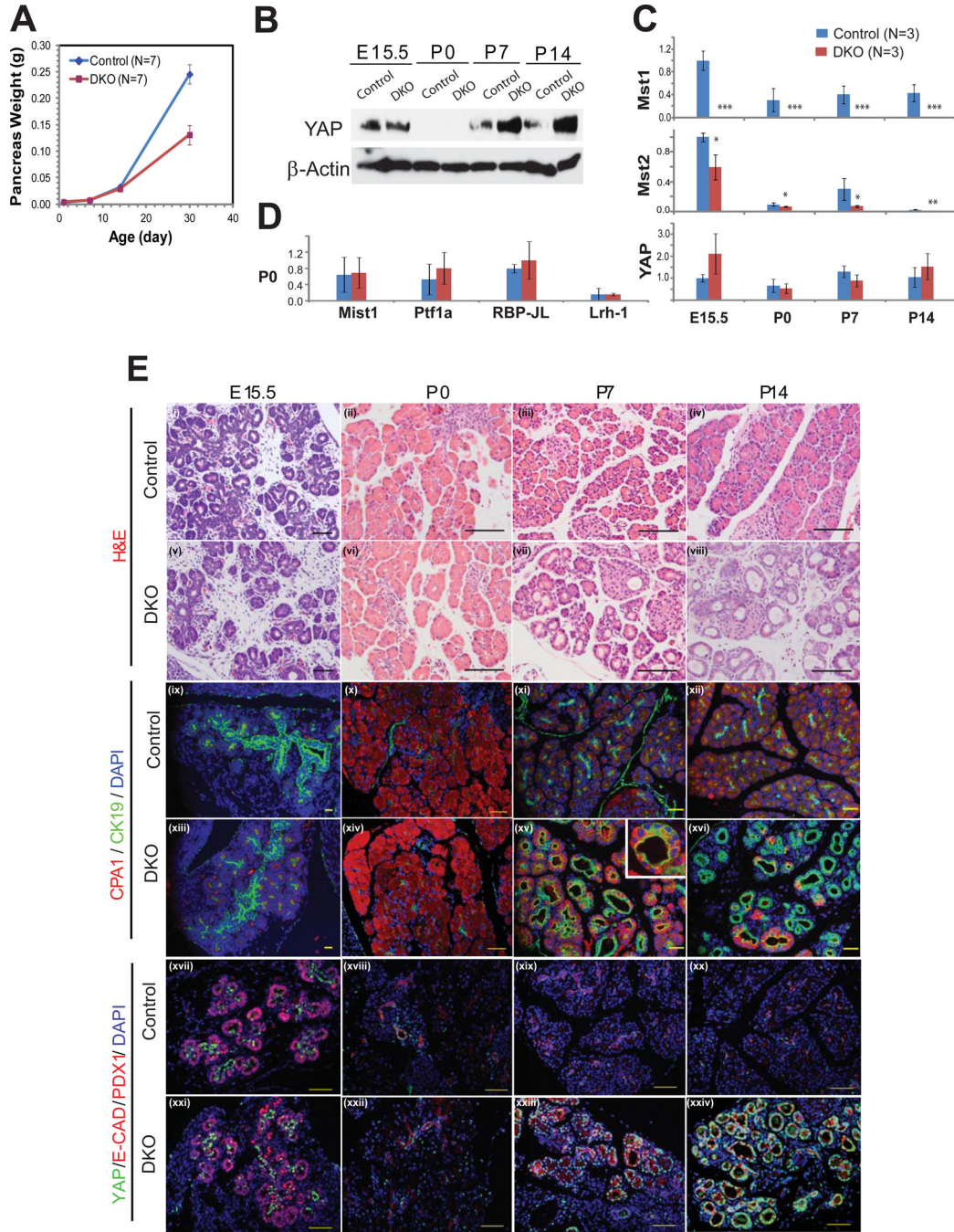


**Figure 3. *Mst1* and *Mst2* are required for postnatal maintenance of the exocrine pancreas**  
 (A) Total pancreas mass of DKO animal was compared to that of littermate controls at P0, P7, P14, and P30 (N=7 per group). A significant difference of body weight was observed on P30 ( $p=0.0013$ ).  
 (B) Western blot assay of pancreas lysates at different time points, starting from E15 through P14, was performed using antibodies against YAP, and  $\beta$ -actin. 30  $\mu$ g of pancreas lysate was loaded per well.  
 (C) qPCR was performed for *Mst1*, *Mst2*, and YAP at each of 4 time-points comparing control and DKO pancreata (n=3 animals in each group per time point). (mean  $\pm$  SD; \*,  $P<0.05$ ; \*\*,  $P<0.01$ ; \*\*\*,  $P<0.001$ ).



(D) qPCR for the acinar transcription factors *Mist1*, *Ptf1a*, *RBP-JL*, and *Lrh-1* were performed at P0 comparing control and DKO pancreata (n=3 animals in each group per time point).

(E) Pancreas tissues of DKO and littermate control were examined by H&E staining (i–viii), immunofluorescence for CK19 and CPA1 (ix–xvi), YAP and PDX1 (xvii,xxi) or YAP and E-Cadherin (xviii–xx, xxii–xxiv) at the indicated developmental stage. Note the strong nuclear YAP staining in the “trunk” regions of both control and DKO embryos at E15.5 and in the duct-like structures of DKO animals at P7 and P14. Scale bar: 100 $\mu$ M.

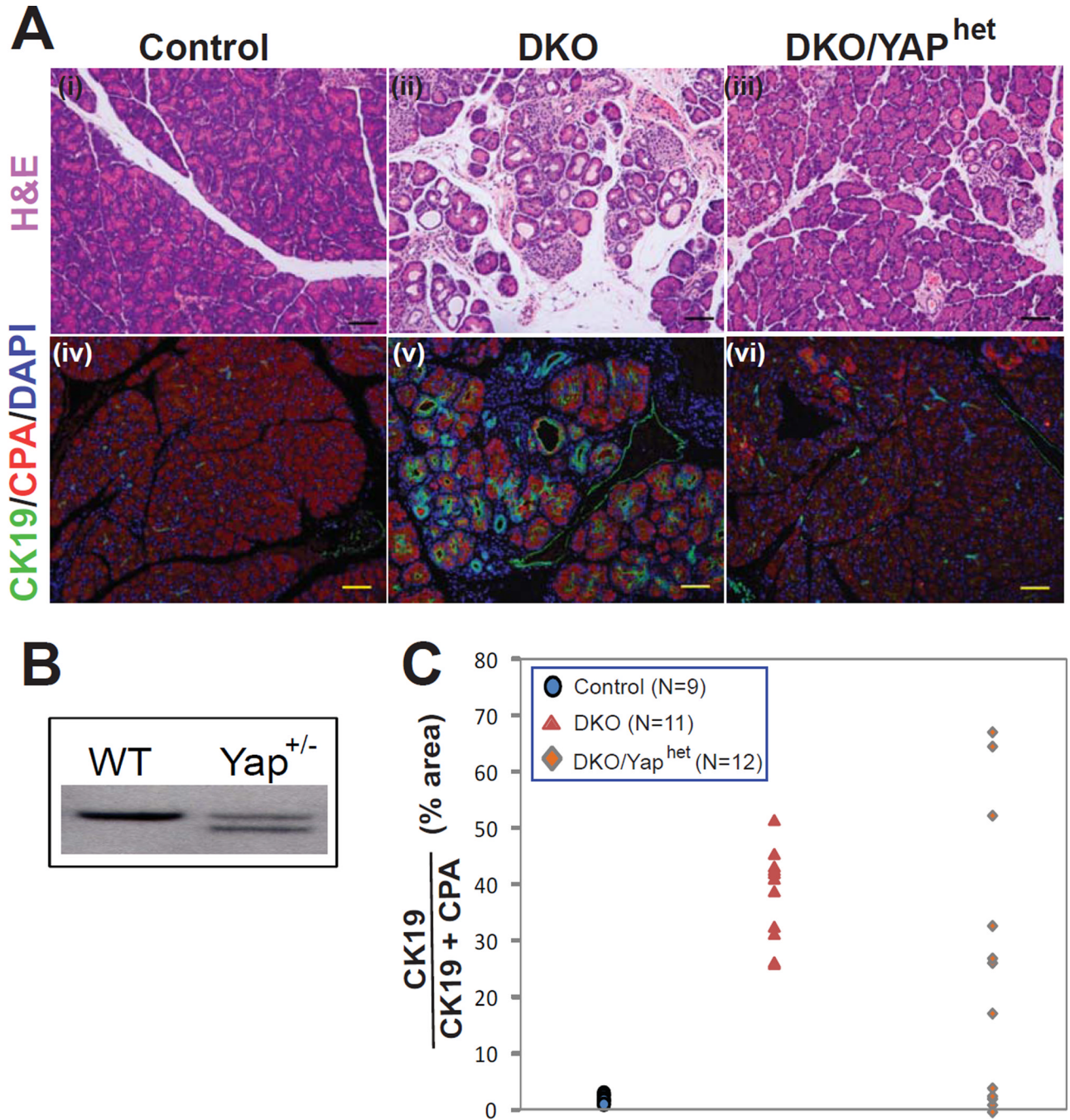


**Figure 4. *Yap* lies downstream of *Mst1/2* in the pancreas**

(A) H&E and immunofluorescence images of P30 control and DKO pancreata showing ductal metaplasia and enhanced CK19 staining (a b d e). In a subset of animals carrying one mutant *Yap* allele, pancreatic histology was normalized despite the absence of *Mst1* and *Mst2* (c f).

(B) Southern blot showing targeting of one *Yap* allele in embryonic stem cells.

(C) Quantification of ductal metaplasia. The area occupied by CK19<sup>+</sup> cells was determined as a percentage of total area occupied by CK19<sup>+</sup> and CPA1<sup>+</sup> cells and plotted. In control animals, CK19<sup>+</sup> cells occupied less than 5%, whereas in DKO animals CK19<sup>+</sup> cells

occupied more than 25%. Four DKO/Yap<sup>het</sup> animals had a complete reversal of metaplasia.  
Scale bar: 100  $\mu$ M.

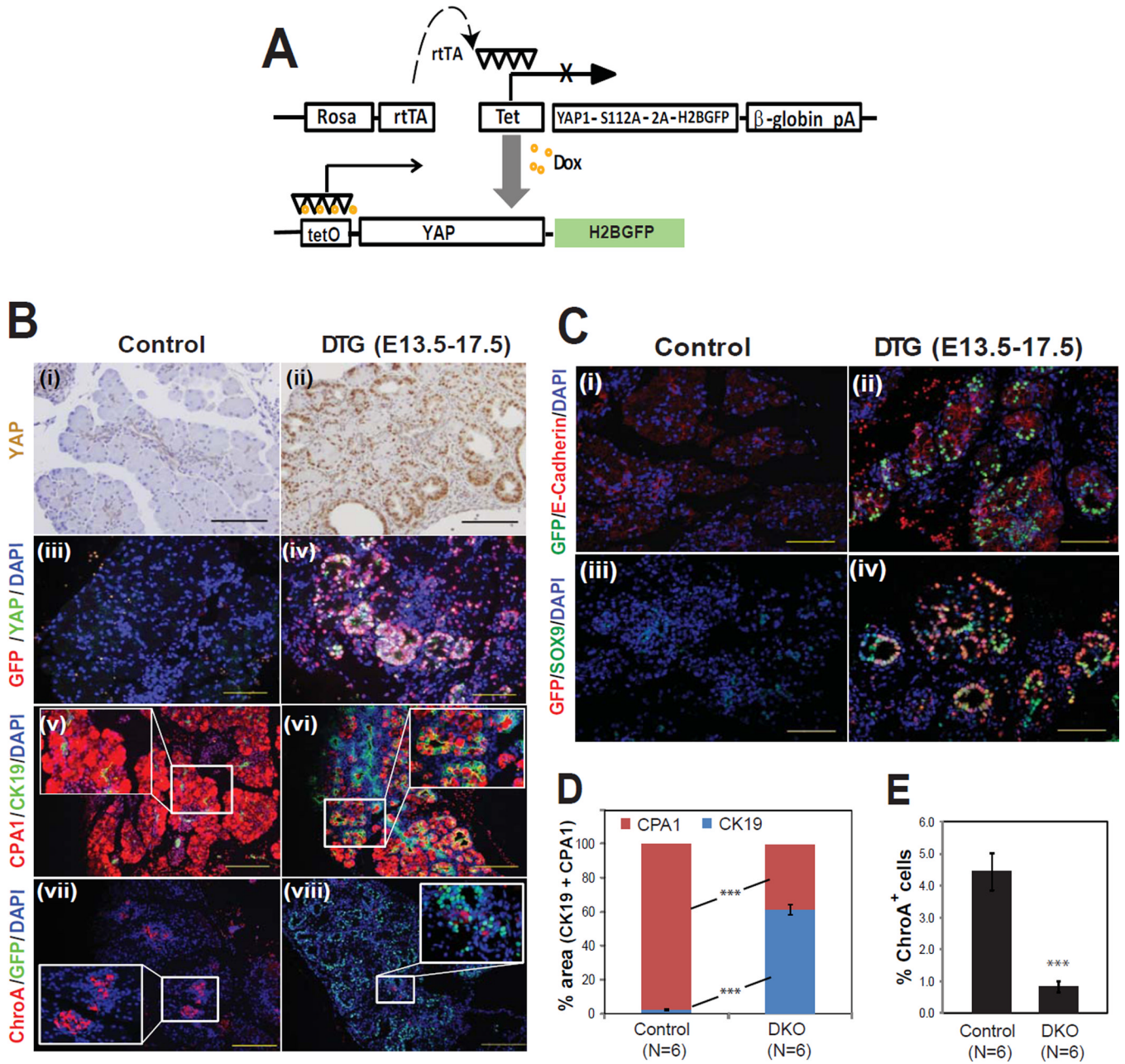


**Figure 5. Reversible activation of YAP in pancreas causes acinar metaplasia and inhibits endocrine differentiation**  
 (A) A tetO-YAP-2A-GFP construct was inserted into the Rosa26 locus by homologous recombination and tetO-YAP-GFP mice were crossed to Rosa-rtTA mice. In bigenic (DTG) mice, transgene expression is dependent upon doxycycline.  
 (B) The YAP-GFP transgene was induced with doxycycline from E13.5 – E17.5 and pancreata were examined at E17.5 by H&E and immunofluorescence for acinar (CPA1), ductal (CK19), and endocrine (ChroA) markers.  
 (C) Co-immunofluorescence for GFP and E-cadherin or Sox9 revealed that transgene expression was most abundant in the epithelium.

(D, E) Quantification of changes in relative percentage of acinar/ductal area (D; measured by CPA1 and CK19 staining) and endocrine area (E; measured by ChroA staining) in control versus DTG pancreata (mean  $\pm$  SD; \*\*\*,  $P < 0.001$ ). Scale bar: 100  $\mu$ M.



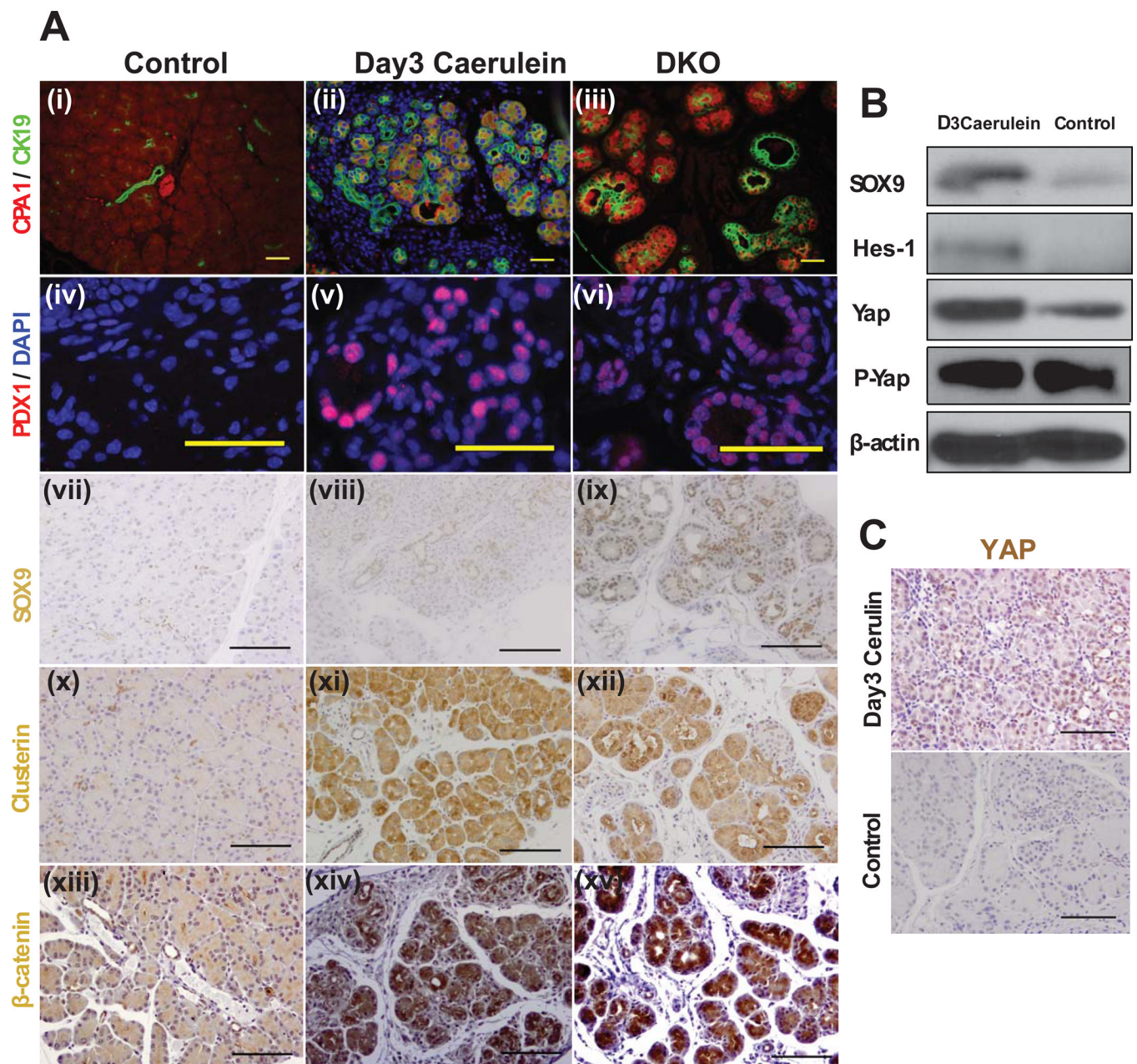


**Figure 6. *Mst1/2* mutation phenocopies acute pancreatitis**

(A) Immunostaining of pancreas from 3 day post-PBS (Control), 3 day post-caerulein (Day3 Caerulein) treated, or 1 month-old DKO mice with antibodies which recognize the indicated proteins.

(B) Proteins were quantified with western blot analysis using 30  $\mu$ g pancreas extracts.

(C) YAP immunostaining of control and caerulein-treated pancreas. Scale bar: 100  $\mu$ M.

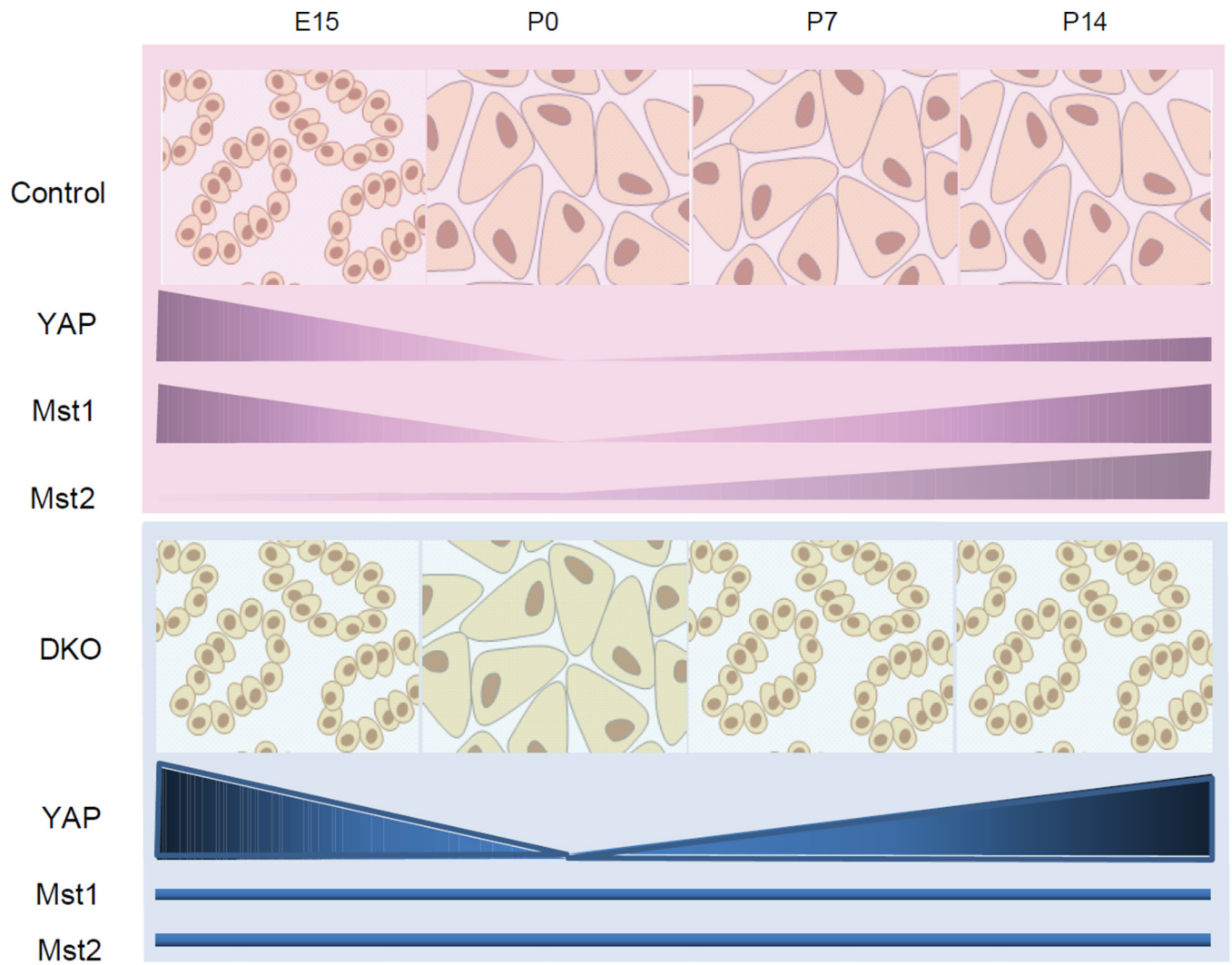


**Figure 7. Model for dynamic regulation of acinar identity by Hippo-YAP signaling**  
See text for detail.